Geophysical Research Letters

RESEARCH LETTER
10.1029/2022GL098385

Record Low Arctic Sea Ice Extent in 2012 Linked to Two-Year La Niña-Driven Sea Surface Temperature Pattern

Hyein Jeong[1], Hyo-Seok Park[1,2], Malte F. Stuecker[3], and Sang-Wook Yeh[1,2]

[1]Institute of Ocean and Atmosphere Science (IOAS), Hanyang University, Ansan, South Korea, [2]Department of Ocean Science and Technology, Hanyang University, Ansan, South Korea, [3]Department of Oceanography & International Pacific Research Center, School of Ocean and Earth Science and Technology, University of Hawai'i at Mānoa, Honolulu, HI, USA

Key Points:

- Tropical sea surface temperature anomalies from 2010 to 2012 played a key role in driving the 2012 record low Arctic sea ice extent (SIE)
- The back-to-back La Niña events during 2010 and 2011 warmed the Arctic Pacific sector
- A negative Pacific Meridional Mode combined with a marginal El Niño in 2012 summer effectively decreased Arctic SIE

Supporting Information:

Supporting Information may be found in the online version of this article.

Correspondence to:

H.-S. Park,
hspark1@gmail.com

Citation:

Jeong, H., Park, H.-S., Stuecker, M. F., & Yeh, S.-W. (2022). Record low Arctic sea ice extent in 2012 linked to two-year La Niña-driven sea surface temperature pattern. *Geophysical Research Letters*, *49*, e2022GL098385. https://doi.org/10.1029/2022GL098385

Received 24 FEB 2022
Accepted 14 APR 2022

Author Contributions:

Conceptualization: Hyein Jeong, Hyo-Seok Park, Malte F. Stuecker, Sang-Wook Yeh
Formal analysis: Hyein Jeong
Funding acquisition: Hyo-Seok Park
Investigation: Hyein Jeong, Malte F. Stuecker
Methodology: Hyein Jeong, Hyo-Seok Park, Malte F. Stuecker
Resources: Hyo-Seok Park
Supervision: Hyo-Seok Park
Validation: Hyein Jeong, Hyo-Seok Park
Visualization: Hyein Jeong
Writing – original draft: Hyein Jeong, Hyo-Seok Park

Abstract Arctic summer sea ice decline accelerated from the mid-2000s to 2012, with the 2012 record low remaining unbroken. While frequent La Niña events during this period have been suggested as a driver of this trend acceleration, no convincing evidence has been presented. Here, using a climate model nudged to observed pan-tropical sea surface temperatures (SST), we show that the back-to-back La Niña events during 2010–2011, followed by a North Pacific cooling and a marginal El Niño, were a key contribution to the 2012 record low. Specifically, the La Niña events in 2010–2011 warmed the Arctic Pacific sector, whereas tropical SST anomalies in 2012 strengthened the Greenland high pressure, leading to an Arctic dipole-like pressure pattern and strengthening of transpolar ice drift. These Arctic temperature and circulation anomalies led to the record low sea ice extent in 2012, highlighting the strong influence of tropical SSTs on Arctic climate.

Plain Language Summary The Arctic summer sea ice cover has been declining over the last decades. The declining trend was particularly rapid from the early 2000's to 2012 with the 2012 record low remaining unbroken. To better understand the mechanism, we carried out several global climate model simulations. We found that relatively cold (2010–2011) equatorial Pacific sea surface temperature (SST) followed by a North Pacific cooling and a weak El Niño-like condition in spring–summer of 2012 played a key role in driving the 2012 record low Arctic sea ice extend. Our model simulations highlight the strong influence of tropical SST on summer Arctic sea ice cover.

1. Introduction

The Arctic has warmed twice as fast as the global average over recent decades with a pronounced decrease in sea ice concentrations. This long-term trend was superimposed by a rapid sea ice loss acceleration from the early 2000's to 2012 (e.g., Ding et al., 2019; Swart et al., 2015). While it has been long recognized that increasing greenhouse gas concentration is the key cause of the declining trend of Arctic sea ice cover (e.g., Goosse et al., 2018; Stuecker et al., 2018), interannual and decadal variations are superimposed on this trend. These fluctuations, or "internal variability", might be responsible for up to 20%–50% of the Arctic sea ice decline over the last three decades (Ding et al., 2017; Kay et al., 2011; Swart et al., 2015). Specifically, the causes of the rapid decline of summer sea ice in 2012 remain to be elucidated.

While synoptic-scale weather events such as intense Arctic cyclones can contribute to rapid sea ice cover decline (Clancy et al., 2022; Parkinson & Comiso, 2013; Zhang et al., 2013), the development of anomalous anticyclonic low-level atmospheric circulation over the pan-Arctic region has been regarded as a major contributor to Arctic summer sea ice loss (Ding et al., 2017; Screen et al., 2011; Wang et al., 2020; Wernli & Papritz, 2018). There is growing evidence that these anticyclonic circulation anomalies are often associated with tropical diabatic heating, which is dynamically tied to tropical sea surface temperature (SST) anomalies on interannual and decadal time scales (Baxter et al., 2019; Bonan & Blanchard-Wrigglesworth, 2020; Ding et al., 2014; Jeong et al., 2022; Lee et al., 2017; Meehl et al., 2018). Specifically, a recent modeling study proposed a physically plausible mechanism explaining how the frequent occurrences of La Niña events could have contributed to the rapid decline of Arctic sea ice from the mid-2000s to 2012 (Baxter et al., 2019). However, their model simulated Arctic sea ice response is rather weak, explaining only about 30%–40% of the observed response. So far, no convincing evidence has been shown that a large fraction of the 2012 record low Arctic sea ice extent (SIE) was driven by tropical climate variability. Using a coupled climate model, we demonstrate that the 2012 record low SIE was driven not only by the back-to-back La Niña events during 2010–2011 but also by a specific tropical SST pattern

Writing – review & editing: Hyein Jeong, Hyo-Seok Park, Malte F. Stuecker, Sang-Wook Yeh

in 2012. Specifically, we present modeling evidence that these tropical SST anomalies can explain about ∼75% of SIE loss and ∼50% of sea ice area reduction for the 2012 September Arctic.

2. Data and Method

2.1. Fully Coupled Model Simulations With CESM2

The Community Earth System Model version 2 (CESM2) was used to identify the impact of tropical SST anomalies on extratropical climate. CESM2 consists of coupled atmosphere (CAM6; Danabasoglu et al., 2020), ocean (POP2; Smith et al., 2010), and sea ice (CICE5; Hunke et al., 2015) components. The horizontal resolution of CAM6 is 1.25° in longitude and 0.9° in latitude. POP2 and CICE5 share the same horizontal resolution, which is a nominal 1° with a uniform resolution of 1.125° in the zonal direction. The meridionally horizontal resolution varies with the finest resolution of 0.27° at the equator. CAM6, POP2, and CICE5 have 32, 60, and 8 vertical levels, respectively. In this study, we performed historical simulations, in which the historical concentrations of anthropogenic greenhouse gases and aerosols as well as volcanic aerosols are prescribed.

2.2. Pacemaker Simulations

We performed pacemaker ensemble simulations forced with tropical SST variability by restoring toward the observed SSTs, using NOAA Optimum Interpolation Sea Surface Temperature (OISST) version 2 (Reynolds et al., 2002), in all three tropical ocean basins between 15°S and 15°N (Figure S1 in Supporting Information S1). The model-simulated tropical SSTs are restored to the observed daily SSTs with a 5-day relaxation time scale. Because the model-simulated SSTs are replaced by seasonally varying daily observed tropical SSTs, tropical SST biases in the model (Li & Xie, 2012; Samanta et al., 2019) are largely removed.

Historical SST simulations for 2010–2012 (*Hist2010–2012*): The model-simulated tropical SSTs are restored to the observed tropical SSTs (15°S–15°N) from April 2010 to September 2013 (hereinafter *Hist2010–2012*).

Historical SST simulations for 2007–2009 (*Hist2007–2009*): The model-simulated tropical SSTs are restored to the observed tropical SSTs from April 2007 to September 2009.

Climatological SST simulations (*Ctrl*): In the control simulation (hereinafter *Ctrl*), the tropical SSTs between 15°S and 15°N are restored to the observed monthly varying climatological SSTs. Considering the increasing tropical SST trend, the climatological mean SSTs both for 2010–2012 and for 2007–2009 are defined as the 2000–2018 average.

Replacing 2012 SSTs with 2009 and 2000 SSTs for the 2010–2012 simulation (*Replace2012by2009* and *Replace2012by2000*): While 1998–2000, 2007–2009, and 2010–2012 experienced back-to-back La Niña events, Arctic summer sea ice decline in 2012 was a lot more pronounced than in 2000 and 2009. To identify the uniqueness of the spring-summer tropical SSTs in 2012 relative to 2000 and 2009 in contributing to the Arctic sea ice loss in September 2012, we designed another two idealized pacemaker simulations (hereinafter *Replace2012by2009* and *Replace2012by2000*). These experiments were branched in March 2012 from the *Hist2010–2012* simulation and tropical SSTs from April 2012 to September 2012 are replaced by SSTs from April 2009 to September 2009 and from April 2000 to September 2000, respectively. As for 2000 spring-summer SSTs, we calculated the linearly detrended monthly mean SST anomalies from 1982 to 2018 and then added SST anomalies of 2000 to the climatological mean SSTs (the 2000–2018 average).

All the pacemaker experiments in this study have 20 ensemble members and each experiment has the same 20 initial conditions. Table S1 in Supporting Information S1 summarizes the detailed information about the pacemaker simulations.

2.3. Reanalysis Data for Validation

The observed SSTs from the OISST (Reynolds et al., 2002) were utilized as a reference. For comparison of atmospheric fields, we used the latest climate reanalysis from the ECMWF (ERA5; Hersbach et al., 2020). To validate the CESM2-simulated SIE, we utilized the satellite-observed SIE provided by the National Snow and Ice Data Center (NSIDC; Fetterer et al., 2017). To calculate SIC, SIE and SST anomalies, we subtracted the

recent 19 years (2000–2018)' climatological means instead of removing the long-term linear trends for a systematic comparison of Arctic sea ice anomalies between our model simulation and observations. As illustrated in Section 2.2, the climatological mean SSTs from 2000 to 2018 are used in our CESM2 pacemaker control simulation (*Ctrl*). Z850, sea level pressure (SLP) and 10 m winds are linearly detrended over 1982–2018 and then the anomalies are calculated by subtracting the long-term (1982–2018) climatological mean. Our results are almost identical even if the recent 19 years (2000–2018)' climatological means are simply subtracted to get the Z850, SLP and 10 m wind anomalies.

A two sample *t*-test was applied for comparing the ensemble-mean Z850 differences between the *Hist2010–2012* and *Ctrl* simulations. The statistically significant values ($p < 0.05$) are stippled in Figure 2c. For the statistical significance of the spatial pattern correlation between ERA5 and our CESM2 simulation, effective degrees of freedom were calculated following the method of Wang and Shen (1999).

3. Results

3.1. Possible Connection Between the Tropical SST Pattern and Arctic SIE

Arctic summer SIE has been declining in recent decades but notable interannual and decadal variations are superimposed on this secular trend (Figure 1a). SIE decrease has accelerated from the early 2000's to 2012, contributing more than 50% of the long-term SIE decline between 1979 and 2020. During 2012 boreal summer Arctic SIE exhibited a record minimum, around $3.5 \times 10^6\ km^2$, with a dramatic recovery in 2013 (Liu & Key, 2014).

The co-occurrence of the rapid decline of SIE from the early 2000s to 2012 with frequent La Niña events during this period has drawn attention to the tropics as a potential driver of this decadal trend (Baxter et al., 2019; Lee, 2012). Figure 1b shows the monthly Niño3.4 index, defined as the normalized SST anomaly averaged over 5°N–5°S and 170°–120°W, from 1979 to 2021. Following the 2009–10 El Niño, La Niña rapidly developed during the 2010 summer and the tropical cold anomalies persisted for about 2 years until the first 3 months of 2012 (Figure 1b). These prolonged La Niña conditions eventually weakened during spring 2012 with a strong negative Pacific Meridional Mode (PMM; Amaya, 2019; Stuecker, 2018) over the North Pacific and with a relatively weak El Niño development following in 2012 summer (Figure 1e). A multi-year La Niña events also happened in 1998–2000 and 2007–2009 (Figure 1b). The SST anomalies during the ensuing summers of these 1998–2000 and 2007–2009 La Niña events however show quite different patterns: La Niña conditions continued in the 2000 summer (Figure 1c), whereas a moderately strong El Niño began to develop in 2009 (Figure 1d).

3.2. Extratropical Circulation Responses to Tropical SSTs

To quantify the impact of the tropical SST anomalies on Arctic climate and sea ice during these years, we performed pacemaker ensemble simulations prescribing the observed SSTs in all three tropical ocean basins in a coupled ocean-atmosphere climate model (see Section 2 for details). Imposing pan-tropical SSTs has the advantage of simulating the observed tropical diabatic heating pattern more accurately (Jeong et al., 2022). The observed non-zonal, 850-hPa geopotential height (Z850) anomalies show that a strong ridge had developed over north-eastern Canada and Greenland, whereas a trough had developed over the Eurasian sector of the Arctic (Figure 2a). Figure 2c shows that the CESM2 pacemaker simulations reproduce the observed Z850 anomalies, a strong ridge over Greenland and a trough over the Eurasian sector of the Arctic. The pattern correlation coefficient of zonal mean excluded Z850 anomalies between the observations and CESM2 simulation is 0.47 ($p < 0.05$) in the northern extratropics (30°N–90°N), highlighting the strong influence of the tropical SST pattern on Arctic circulation anomaly in 2012 summer.

The dipole pattern of Z850 anomalies in the Arctic was accompanied by anomalous high pressure over the north-eastern Canada–Greenland sector and low pressure over the Pacific sector of the Arctic (Figure 2b). Satellite-observed sea ice motion anomalies show that this dipole SLP pattern strengthened the transpolar sea ice drift toward the Fram Strait, especially during the early summer (June–July; Figure S2 in Supporting Information S1), which has been suggested as a favorable condition for accelerating summer sea ice loss (Ding et al., 2017; Smedsrud et al., 2017). Our CESM2 pacemaker experiment simulates the dipole SLP pattern (Figure 2d) and the strengthening of transpolar sea ice drift (Figure S2 in Supporting Information S1). The CESM2 simulation, however, does not reproduce the cyclonic circulation anomaly over the Chukchi–East Siberian Seas (Figure 2b vs. 2d) because

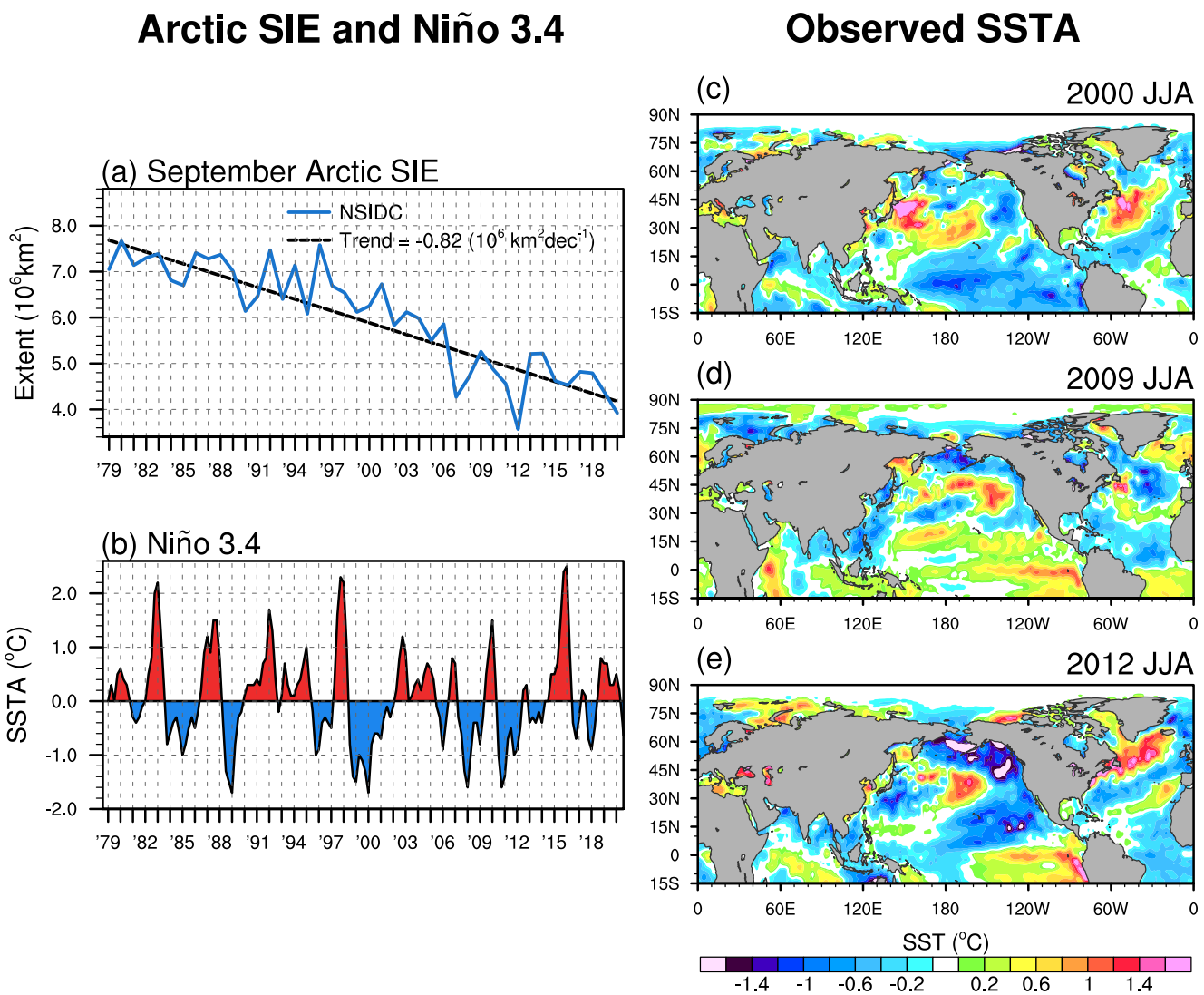

Figure 1. (a) September Arctic sea ice extent (10^6 km^2) of National Snow and Ice Data Center (NSIDC) satellite observations from 1979 to 2020 (blue line). The black-dashed line in (a) is a linear regression line for September sea ice extent. (b) Monthly Niño3.4 index (°C) from January 1979 to February 2021. Observed sea surface temperature (°C) anomaly during the summers of (c) 2000, (d) 2009, and (e) 2012.

the CESM2 experiment does not reproduce the exceptionally strong Arctic cyclone event in the early August of 2012, likely attributable to internal variability.

The extratropical circulation anomalies during the La Niña summers of 2010 and 2011 are also captured by our CESM2 pacemaker simulation. For the 2010–11 summer average, our model-simulated Z850 anomalies are partly corroborated by observed Z850 anomalies (Figure S3 in Supporting Information S1): the pattern correlation coefficient of zonal mean excluded Z850 anomalies between the observations and CESM2 simulation is 0.42 ($p < 0.05$) in the northern extratropics (30°N–90°N). The anomalously high Z850 over the Pacific sector of the Arctic are accompanied by anomalous lower tropospheric warming and the development of high SLP anomalies (Figure S3 in Supporting Information S1). The strengthening of the surface anticyclone over the Beaufort Sea, which can strengthen downward shortwave radiation and the transpolar sea ice drift, has long been regarded as one of the key circulation patterns accelerating the summer sea ice loss (Knudsen et al., 2015; Wang et al., 2020; Wernli & Papritz, 2018).

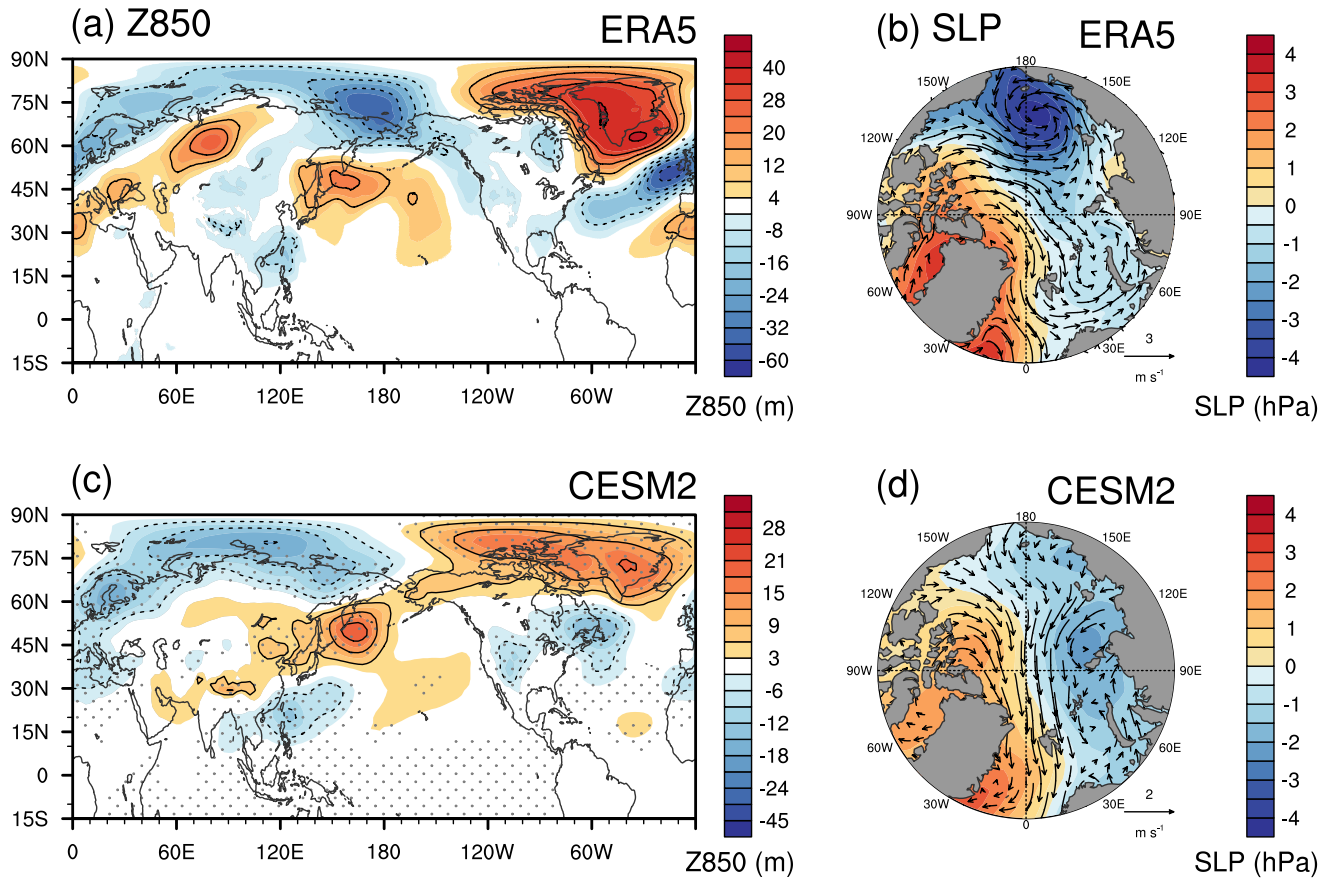

Figure 2. (a,c) Non-zonal component of 850 hPa geopotential height (m) anomalies and (b,d) Sea Level Pressure (hPa) with 10 m wind anomalies in the summer of 2012 for (upper; a,b) ERA5 reanalysis and (bottom: c,d) Community Earth System Model version 2 (CESM2) experiment ensemble-mean (*Hist2010–2012*). For the CESM2 experiment, the statistical significance of each grid point is calculated from the difference between *Hist2010–2012* and *Ctrl* simulations (20 ensemble members each). In (c), statistically significant values ($p < 0.05$), calculated from two sample *t*-test, are stippled.

3.3. Arctic Sea Ice Responses to Tropical SSTs

In response to the changes in Arctic atmospheric circulation and temperatures, Arctic summer sea ice cover rapidly declined. Figure 3 shows the sea ice concentration (SIC) anomalies in satellite observations and in our CESM2 simulation. During La Niña summers, the observed SIC decreased along the marginal ice zone by around 10%–20% in September 2010 and 2011 (Figures 3a and 3b). The associated September SIE anomalies were about 0.32 and $0.63 \times 10^6\ km^2$ lower than average in 2010 and 2011, respectively (red line in Figure 3g). Consistent with the satellite observations, CESM2 forced with observed tropical SSTs generally reproduces the decreased summer SIC along the marginal ice zones in 2010 and 2011 (Figures 3d and 3e). However, it is worth noting that the detailed spatial patterns of SIC anomalies between the observations and the CESM2 simulation are somewhat different from each other. These differences can most likely be explained by some notable differences in the sea ice drift anomalies between the observations and CESM2 simulation (Figure S2 in Supporting Information S1), which can have a strong influence on sea ice concentrations.

In September 2012, the SIC anomalies were drastically reduced (Figure 3c), leading to $\sim 1.6 \times 10^6\ km^2$ lower than average SIE (red line in Figure 3g), which is still an unbroken record. The CESM2 forced with observed tropical SSTs simulates the dramatic reduction of summer SIE anomaly in 2012 (Figure 3g). Although the ensemble spread in the model simulation is relatively large in the summer (thin black lines in Figure 3g), the ensemble-mean monthly SIE anomalies match well with the observations. The correlation coefficient of monthly mean SIE anomalies from January 2010 to September 2013 between the observations and our model simulation is 0.62 ($p < 0.01$). Our model-simulated SIE anomaly in September 2012 is about $-1.2 \times 10^6\ km^2$, explaining

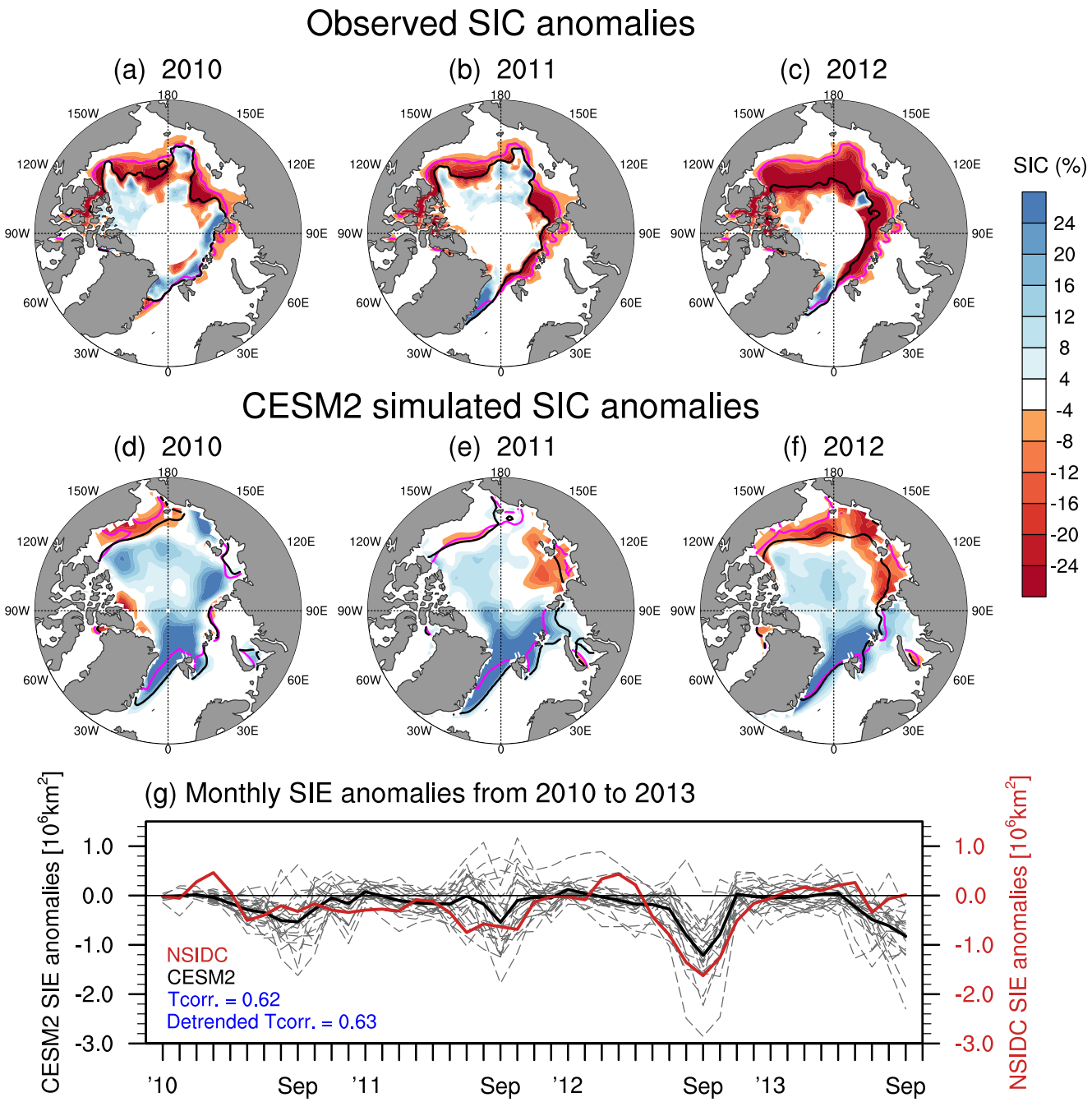

Figure 3. September sea ice concentration (%) anomalies in (a,d) 2010 (b,e) 2011, and (e,f) 2012, for (a–c) National Snow and Ice Data Center (NSIDC) satellite observations and (d–f) the Community Earth System Model version 2 (CESM2) experiment ensemble-mean (*Hist2010–2012*). For the NSIDC satellite observations, the sea ice concentration anomalies are relative to the 2000–2018 climatology. For the CESM2 simulation, statistically significant values ($p < 0.05$) are stippled. Pink solid lines denote the September climatological-mean sea ice edges (15% concentration). Black solid lines indicate the 15% September sea ice concentration contours for specific years. (g) Monthly sea ice extend anomalies from 2010 to 2013 calculated from NSIDC satellite observations (red line) and the CESM2 simulations (black line: ensemble average, gray dashed lines: each ensemble member).

more than 75% of the observed reduction of SIE $-1.6 \times 10^6\ km^2$. In the meanwhile, CESM2-simulated sea ice area anomaly in September 2012 is $-0.7 \times 10^6\ km^2$ and this is about 55% of the observed reduction of sea ice area anomaly, which is $-1.23 \times 10^6\ km^2$. The underestimation of the sea ice area reduction in September 2012 is because CESM2 does not capture the observed reduction of SIC over the Beaufort Sea (Figures 3c and 3f).

Although the ensemble-mean summer sea ice response is somewhat smaller than the observations, three ensembles out of 20 ensemble members simulate larger decline of September SIE than the observations (see black-dotted lines in Figure 3g). One standard deviation of our model-simulated September SIE anomalies calculated from 20 ensemble members is about $0.63 \times 10^6\ km^2$, which may represent the internal variability. Therefore, we infer that the sum of the forced response (ensemble average) and the internal variability can be as low as $-1.2 \times 10^6 - 0.63 \times 10^6 = -1.84 \times 10^6\ km^2$.

3.4. Differences Between 2010–2012 and 2007–2009

The above results raise question of why tropical SST anomalies during 2010–2012 are special to drive the record sea ice loss in 2012 summer. Since the early 2000's, the back-to-back La Niña events not only happened in 2010–2011 but also in 2007–2008 (Figure 1b). Unlike 2010–2012, the back-to-back La Niña in 2007–2008 was not followed by a notable decline of September SIE in 2009 (Figure 1a). To elucidate the difference between 2010–2012 and 2007–2009, we performed another pacemaker simulation by restoring pan-tropical SSTs from April 2007 to September 2009 (see Section 2 for details).

Our model simulated extratropical Z850 anomalies in 2009 are very different from those of 2012 (Figure 4). The dipole pattern of Z850 anomalies in 2012 summer (Figures 2a, 2c and 4a), does not appear in 2009 in the Arctic (Figure 4b). The North Pacific SST responses are also different from each other (Figures 4d and 4e). Our pacemaker simulation for 2010–2012 leads to an SST pattern that has characteristics of a negative phase of PMM in the 2012 summer (Figure 4d), which is generally consistent with the observations (Figure 1e) and expected from a strong La Niña forcing (Stuecker, 2018). However, the back-to-back La Niña in 2007–2008 does not lead to a clear negative PMM pattern in the 2009 summer over the North Pacific (Figure 4e).

These differences in extratropical SST and circulation anomalies between 2012 and 2009 are also accompanied by the differences in Arctic SIE. Figures 4g and 4h show monthly SIE anomaly in each ensemble for 2012 and 2009, respectively. The gray shadings indicate the one standard deviation range of monthly SIE anomaly calculated from the control simulation (*Ctrl*) with 20 ensembles. Both pacemaker experiments including *Hist2010–2012* and *Hist2007–2009* simulate anomalously low summer SIE in 2012 and 2009, suggesting that the back-to-back La Niña events provide favorable condition for sea ice decline in the subsequent summer. However, 2012 summer sea ice loss is more pronounced than in 2009. In September 2012, 14 out of 20 ensemble members exceed the internal variability (gray shading) and two ensembles end up with extremely low SIE (Figure 4g). In 2009 September, 8 out of 20 ensemble members exceed the internal variability (Figure 4h).

3.5. The Effectiveness of 2012 Summer SST in Driving Rapid Arctic Sea Ice Decline

We hypothesize that a slightly different tropical Pacific SST anomaly pattern in 2012, which exhibits both a negative PMM and a marginal El Niño, played a key role in driving rapid Arctic sea ice decline. To test this hypothesis, we performed two idealized pacemaker simulations: for the 2010–2012 historical pacemaker simulation (*Hist2010–2012*), the tropical SSTs from April to September are replaced by the 2009 tropical SSTs (*Replace2012by2009*) and by 2000 tropical SSTs (*Replace2012by2000*). In *Replace2012by2009* experiment, the North Pacific cooling substantially weakens (Figure 5b), whereas, both the La Niña condition and a negative PMM-like North Pacific cooling appear in the *Replace2012by2000* experiment (Figure 5c).

In *Replace2012by2009* and *Replace2012by2000* experiments, the Arctic sea ice declines less rapidly (Figures 5e and 5f): while the ensemble-mean September SIE anomaly is still significantly low, 15 out of 20 ensemble members are within the range of internal variability in both experiments. Box plots of September SIE anomalies clearly show that the tropical SSTs decreased September Arctic SIE more effectively in 2012 than in 2000 and 2009 (Figure 5g). These results suggest that the consecutive La Niña events during 2010–2011 followed by a North Pacific cooling and a marginal El Niño in 2012 summer were a key driver of the summer Arctic sea ice loss. Our model simulated results are also consistent with a recent observational analysis (Baxter et al., 2019), which found that the tropics-to-Arctic linkage was particularly strong from 2010 to 2012.

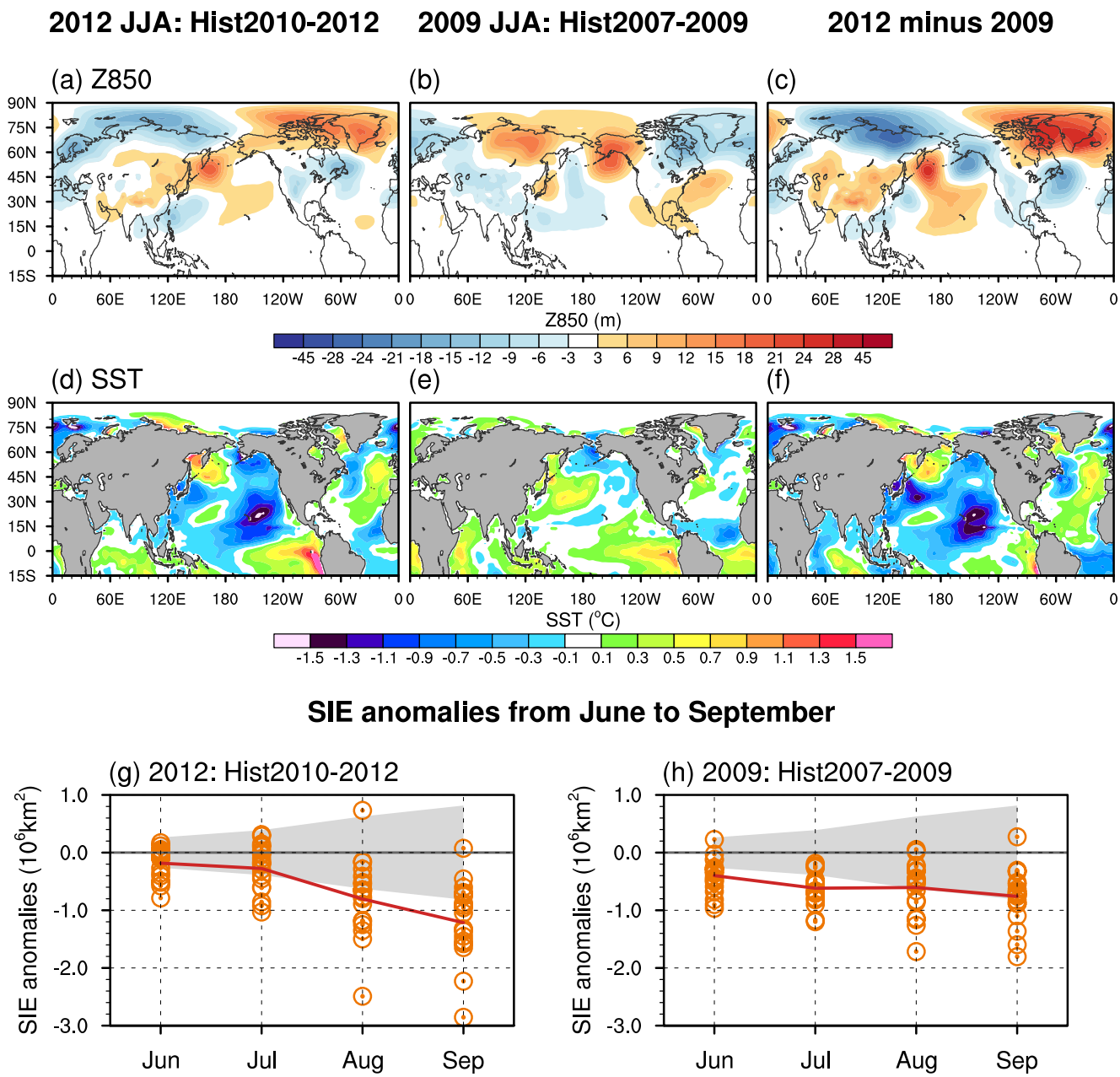

Figure 4. (a–c) Non-zonal component of 850 hPa geopotential height (m) anomalies and (d–f) sea surface temperature (°C) anomalies (left; a,d) in 2012 summer from *Hist2010–2012* (middle; b,e) in 2009 summer from *Hist2007–2009*, and (right; c,f) differences between two simulations. Monthly sea ice extend (SIE) anomalies calculated from the Community Earth System Model version 2 simulation (red line: ensemble average, orange markers: each ensemble member, gray shading: ±1 standard deviation range of SIE anomalies from control simulation) from June to September in (g) 2012 from *Hist2010–2012* and (h) 2009 from *Hist2007–2009*.

4. Summary

By nudging observed tropical SSTs in a state-of-the-art coupled climate model, we identified the impact of tropical SST anomalies on the 2012 record low Arctic SIE. In the case when the tropical SSTs from 2010 to 2012 are nudged to the observations in the model, the dramatic Arctic sea ice loss in 2012 summer is reproduced well. Specifically, our model simulation demonstrates that La Niña conditions in the summer of 2010 and 2011 increased lower tropospheric temperature over the Pacific sector of the Arctic, whereas a negative phase of PMM in 2012 strengthened the anomalous Greenland high and the associated transpolar drift of sea ice toward the Fram Strait.

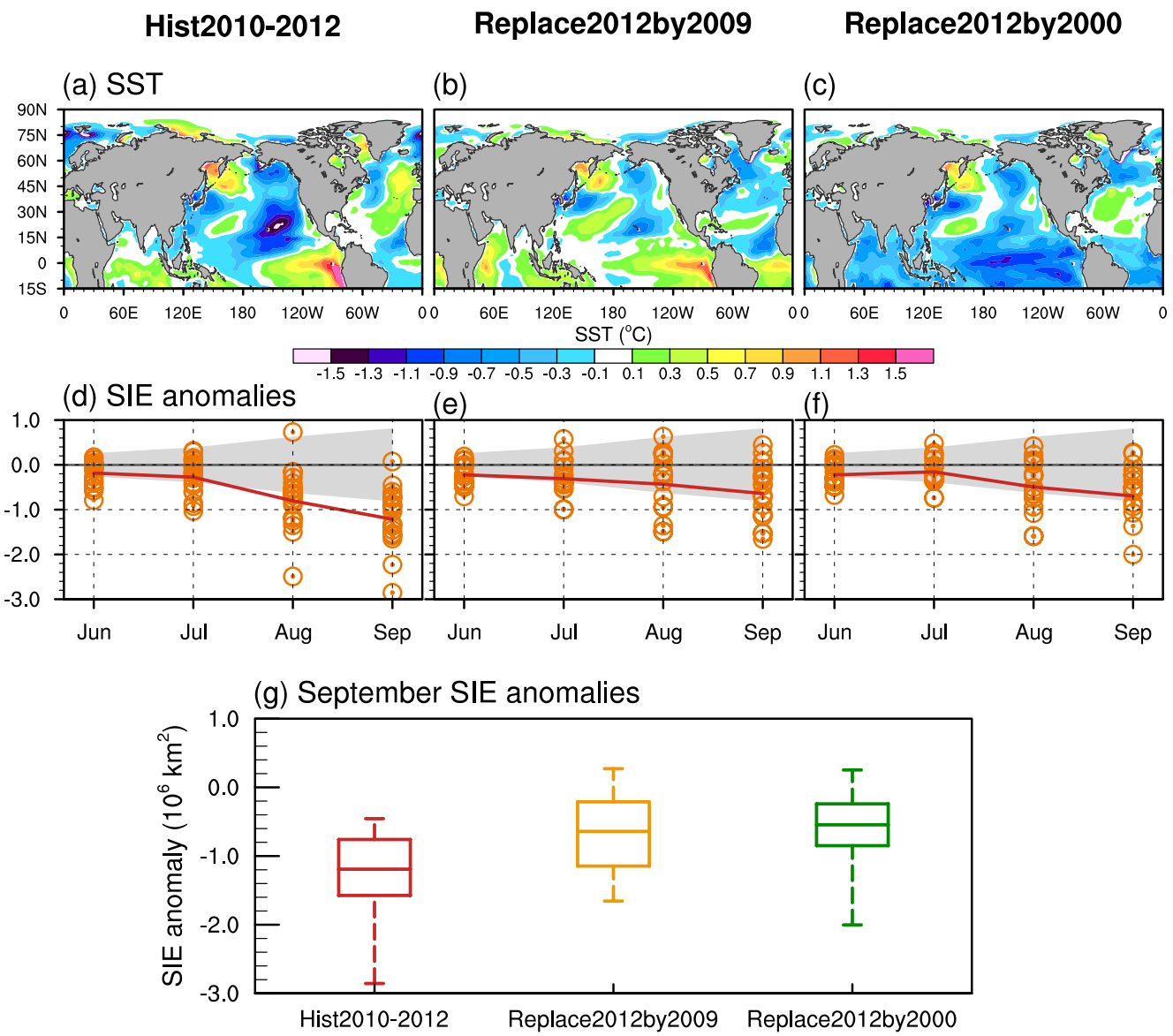

Figure 5. (a–c) Sea surface temperature (°C) anomalies in 2012 summer (JJA) in (a) *Hist2010-2012*, (b) *Replace2012by2009*, and (c) *Replace2012by2000* (d–f) Monthly sea ice extend (SIE) anomalies calculated from the Community Earth System Model version 2 (CESM2) simulation (red line: ensemble average, orange markers: each ensemble member, gray shading: ±1 standard deviation range of SIE anomalies from the control simulation) from June to September in 2012 from (d) *Hist2010–2012,* (e) *Replace2012by2009,* and (f) *Replace2012by2000.* (g) Box plots for ensemble mean and ensemble spread of CESM2-simulated SIE anomalies in September 2012 from *Hist2010–2012* (red), *Replace2012by2009* (yellow), and *Replace2012by2000* (green). Shown in each box plot are the median (middle solid line), the 25th and 75th percentiles (lower and upper hinge), and the 5th and 95th percentiles (whiskers) of 20 ensemble members. Figures 5a and 5d are identical to Figures 4d and 4g.

Numerous previous studies have examined potential causes of summer Arctic SIE variations superimposed on the secular trend with recent studies suggesting that tropical SST anomalies can contribute to these variations (e.g., Baxter et al., 2019; Ding et al., 2017). This study demonstrates that consecutive La Niña events followed by a negative PMM and marginal El Niño were the optimal tropical SST pattern contributing to the rapid sea ice decline from 2010 to 2012. This insight will not only help improve our understanding of tropics-to-Arctic teleconnections but also help assess the potential predictability of summer Arctic sea ice cover on interannual and decadal time scales.

Data Availability Statement

Monthly climate model outputs for CESM2 pacemaker simulations conducted for the purpose of this study can be downloaded from Data Dryad: https://doi.org/10.5061/dryad.s1rn8pk90. ERA5 reanalysis data can be downloaded from the Copernicus repository https://cds.climate.copernicus.eu/cdsapp#!/dataset/reanalysis-era5-pressure-levels-monthly-means?tab=form. Optimum Interpolation Sea Surface Temperature version 2 data provided at https://psl.noaa.gov/data/gridded/data.noaa.oisst.v2.html. Sea ice concentration from NSIDC can be obtained from https://nsidc.org/data/G02202/versions/4. Sea ice motion vectors from NSIDC can be delivered from https://nsidc.org/data/NSIDC-0116/versions/4.

Acknowledgments
The authors thank four anonymous reviewers for helpful and constructive comments. The main calculations were performed by the supercomputing resource of the Korea Meteorological Administration (National Center for Meteorological Supercomputer). This research was supported by the National Research Foundation of Korea (NRF) no. 2020R1A2C2010025. MFS was supported by NOAA's Climate Program Office's Modeling, Analysis, Predictions, and Projections (MAPP) program grant NA20OAR4310445. This is IPRC publication 1563 and SOEST contribution 11505.

References

Amaya, D. J. (2019). The Pacific meridional mode and ENSO: A review. *Current Climate Change Reports*, *5*(4), 296–307. https://doi.org/10.1007/s40641-019-00142-x

Baxter, I., Ding, Q., Schweiger, A., L'Heureux, M., Baxter, S., Wang, T., et al. (2019). How tropical Pacific surface cooling contributed to accelerated sea ice melt from 2007 to 2012 as ice is thinned by anthropogenic forcing. *Journal of Climate*, *32*(24), 8583–8602. https://doi.org/10.1175/jcli-d-18-0783.1

Bonan, D. B., & Blanchard-Wrigglesworth, E. (2020). Nonstationary teleconnection between the Pacific Ocean and Arctic sea ice. *Geophysical Research Letters*, *47*(2), e2019GL085666. https://doi.org/10.1029/2019gl085666

Clancy, R., Bitz, C. M., Blanchard-Wrigglesworth, E., McGraw, M. C., & Cavallo, S. M. (2022). A cyclone-centered perspective on the drivers of asymmetric patterns in the atmosphere and sea ice during Arctic cyclones. *Journal of Climate*, *35*(1), 73–89. https://doi.org/10.1175/jcli-d-21-0093.1

Danabasoglu, G., Lamarque, J. F., Bacmeister, J., Bailey, D. A., DuVivier, A. K., Edwards, J., et al. (2020). The community Earth system model version 2 (CESM2). *Journal of Advances in Modeling Earth Systems*, *12*(2), e2019MS001916. https://doi.org/10.1029/2019ms001916

Ding, Q., Schweiger, A., L'Heureux, M., Battisti, D. S., Po-Chedley, S., Johnson, N. C., et al. (2017). Influence of high-latitude atmospheric circulation changes on summertime Arctic sea ice. *Nature Climate Change*, *7*(4), 289–295. https://doi.org/10.1038/nclimate3241

Ding, Q., Schweiger, A., L'Heureux, M., Steig, E. J., Battisti, D. S., Johnson, N. C., et al. (2019). Fingerprints of internal drivers of Arctic sea ice loss in observations and model simulations. *Nature Geoscience*, *12*(1), 28–33. https://doi.org/10.1038/s41561-018-0256-8

Ding, Q., Wallace, J. M., Battisti, D. S., Steig, E. J., Gallant, A. J., Kim, H. J., & Geng, L. (2014). Tropical forcing of the recent rapid Arctic warming in northeastern Canada and Greenland. *Nature*, *509*(7499), 209–213. https://doi.org/10.1038/nature13260

Fetterer, F., Knowles, K., Meier, W. N., Savoie, M., & Windnagel, A. K. (2017). *Sea Ice index, version 3*. Updated daily. NSIDC: National Snow and Ice Data Center. https://doi.org/10.7265/N5K072F8

Goosse, H., Kay, J. E., Armour, K. C., Bodas-Salcedo, A., Chepfer, H., Docquier, D., et al. (2018). Quantifying climate feedbacks in polar regions. *Nature Communications*, *9*, 1–13. https://doi.org/10.1038/s41467-018-04173-0

Hersbach, H., Bell, B., Berrisford, P., Hirahara, S., Horányi, A., Muñoz-Sabater, J., et al. (2020). The ERA5 global reanalysis. *Quarterly Journal of the Royal Meteorological Society*, *146*(730), 1999–2049. https://doi.org/10.1002/qj.3803

Hunke, E. C., Lipscomb, W. H., Turner, A. K., Jeffery, N., & Elliott, S. (2015). Cice: The Los Alamos Sea Ice model. Documentation and software user's manual. Version 5.1. *T-3 fluid dynamics group. Los Alamos National Laboratory*. Technical Report LA-CC-06-012.

Jeong, H., Park, H. S., Stuecker, M. F., & Yeh, S. W. (2022). Distinct impacts of major El Niño events on Arctic temperatures due to differences in eastern tropical Pacific sea surface temperatures. *Science Advances*, *8*(4), 1–11. https://doi.org/10.1126/sciadv.abl8278

Kay, J. E., Holland, M. M., & Jahn, A. (2011). Inter-annual to multi-decadal Arctic sea ice extent trends in a warming world. *Geophysical Research Letters*, *38*(15). https://doi.org/10.1029/2011gl048008

Knudsen, E. M., Orsolini, Y. J., Furevik, T., & Hodges, K. I. (2015). Observed anomalous atmospheric patterns in summers of unusual Arctic sea ice melt. *Journal of Geophysical Research: Atmospheres*, *120*(7), 2595–2611. https://doi.org/10.1002/2014jd022608

Lee, M. H., Lee, S., Song, H.-Y., & Ho, C.-H. (2017). The recent increase in the occurrence of a boreal summer teleconnection and its relationship with temperature extremes. *Journal of Climate*, *30*(18), 7493–7504. https://doi.org/10.1175/jcli-d-16-0094.1

Lee, S. (2012). Testing of the tropically excited Arctic warming mechanism (TEAM) with traditional El Niño and La Niña. *Journal of Climate*, *25*(12), 4015–4022. https://doi.org/10.1175/jcli-d-12-00055.1

Li, G., & Xie, S. P. (2012). Origins of tropical-wide SST biases in CMIP multi-model ensembles. *Geophysical Research Letters*, *39*(22). https://doi.org/10.1029/2012gl053777

Liu, Y., & Key, J. R. (2014). Less winter cloud aids summer 2013 Arctic sea ice return from 2012 minimum. *Environmental Research Letters*, *9*(4), 044002. https://doi.org/10.1088/1748-9326/9/4/044002

Meehl, G. A., Chung, C. T. Y., Arblaster, J. M., Holland, M. M., & Bitz, C. M. (2018). Tropical decadal variability and the rate of Arctic sea ice decrease. *Geophysical Research Letters*, *45*(20), 11326–11333. https://doi.org/10.1029/2018gl079989

Parkinson, C. L., & Comiso, J. C. (2013). On the 2012 record low Arctic sea ice cover: Combined impact of preconditioning and an August storm. *Geophysical Research Letters*, *40*(7), 1356–1361. https://doi.org/10.1002/grl.50349

Reynolds, R. W., Rayner, N. A., Smith, T. M., Stokes, D. C., & Wang, W. (2002). An improved in situ and satellite SST analysis for climate. *Journal of Climate*, *15*(13), 1609–1625. https://doi.org/10.1175/1520-0442(2002)015<1609:aiisas>2.0.co;2

Samanta, D., Karnauskas, K. B., & Goodkin, N. F. (2019). Tropical Pacific SST and ITCZ biases in climate models: Double trouble for future rainfall projections? *Geophysical Research Letters*, *46*(4), 2242–2252. https://doi.org/10.1029/2018gl081363

Screen, J. A., Simmonds, I., & Keay, K. (2011). Dramatic interannual changes of perennial Arctic sea ice linked to abnormal summer storm activity. *Journal of Geophysical Research: Atmospheres*, *116*(D15), D15105. https://doi.org/10.1029/2011jd015847

Smedsrud, L. H., Halvorsen, M. H., Stroeve, J. C., Zhang, R., & Kloster, K. (2017). Fram Strait sea ice export variability and September Arctic sea ice extent over the last 80 years. *The Cryosphere*, *11*(1), 65–79. https://doi.org/10.5194/tc-11-65-2017

Smith, R., Jones, P., Briegleb, B., Bryan, F., Danabasoglu, G., Dennis, J., et al. (2010). The parallel ocean program (POP) reference manual, ocean component of the community climate system model (CCSM), LANL Technical Report, LAUR-10-01853, 141.

Stuecker, M. F. (2018). Revisiting the Pacific meridional mode. *Scientific Reports*, *8*(1), 1–9. https://doi.org/10.1038/s41598-018-21537-0

Stuecker, M. F., Bitz, C. M., Armour, K. C., Proistosescu, C., Kang, S. M., Xie, S. P., et al. (2018). Polar amplification dominated by local forcing and feedbacks. *Nature Climate Change*, *8*(12), 1076–1081. https://doi.org/10.1038/s41558-018-0339-y

Swart, N. C., Fyfe, J. C., Hawkins, E., Kay, J. E., & Jahn, A. (2015). Influence of internal variability on Arctic sea-ice trends. *Nature Climate Change*, *5*(2), 86–89. https://doi.org/10.1038/nclimate2483

Wang, X., & Shen, S. S. (1999). Estimation of spatial degrees of freedom of a climate field. *Journal of Climate*, *12*(5), 1280–1291. https://doi.org/10.1175/1520-0442(1999)012<1280:eosdof>2.0.co;2

Wang, Z., Walsh, J., Szymborski, S., & Peng, M. (2020). Rapid Arctic sea ice loss on the synoptic time scale and related atmospheric circulation anomalies. *Journal of Climate*, *33*(5), 1597–1617. https://doi.org/10.1175/jcli-d-19-0528.1

Wernli, H., & Papritz, L. (2018). Role of polar anticyclones and mid-latitude cyclones for Arctic summertime sea-ice melting. *Nature Geoscience*, *11*(2), 108–113. https://doi.org/10.1038/s41561-017-0041-0

Zhang, J., Lindsay, R., Schweiger, A., & Steele, M. (2013). The impact of an intense summer cyclone on 2012 Arctic sea ice retreat. *Geophysical Research Letters*, *40*(4), 720–726. https://doi.org/10.1002/grl.50190